

CATALOGED BY DDC
AS AD NO. 1

426201

Report No. 1
First Quarterly Report

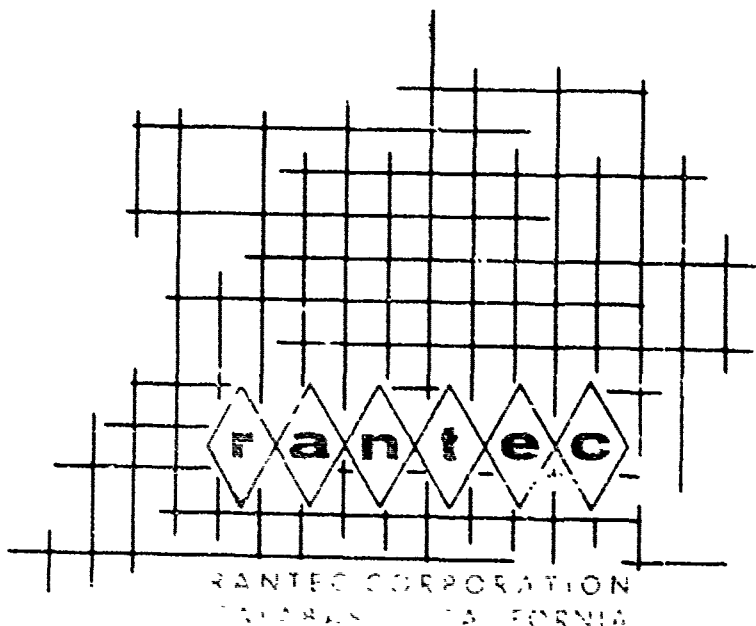
Covering the Period
1 July 1963 to 30 September 1963

**Investigation of
MICROWAVE DIELECTRIC-RESONATOR FILTERS**

Prepared for:
U. S. ARMY ELECTRONICS RESEARCH AND DEVELOPMENT LABORATORY
FORT MONMOUTH, NEW JERSEY

CONTRACT DA 36-039-AMC-02267(E)
TASK NO. 5544-PM-63-91

By: S. B. Cohn and G. W. Chandler



Report No. 1
First Quarterly Report

Covering the Period
1 July 1963 to 30 September 1963

Investigation of
MICROWAVE DIELECTRIC-RESONATOR FILTERS


Prepared for:
U. S. ARMY ELECTRONICS RESEARCH AND DEVELOPMENT LABORATORY
FORT MONMOUTH, NEW JERSEY

CONTRACT DA 36-039-AMC-02267(E)
TASK NO. 5544-PM-63-91

By: S. B. Cohn and C. W. Chandler

Ranec Project No. 31625

Approved:



SEYMOUR B. COHN, Technical Director

TABLE OF CONTENTS

SECTION	TITLE	PAGE
I	PURPOSE	1
II	ABSTRACT	2
III	CONFERENCES	3
IV	FACTUAL DATA	4
	Introduction	4
	First- and Second-Order Analysis of Dielectric Resonators	9
	First-Order Solution	9
	Impedance Discontinuity on an Infinite Plane Boundary	10
	Second-Order Solution	13
	Comparison of First- and Second-Order Solutions with Measured Data	17
	Measurements on Cylindrical Dielectric Resonators	19
V	CONCLUSIONS	24
VI	PROGRAM FOR NEXT INTERVAL	25
VII	LIST OF REFERENCES	26
VIII	IDENTIFICATION OF KEY TECHNICAL PERSONNEL	27
	ASTIA CARDS	28

LIST OF ILLUSTRATIONS

FIGURE	TITLE	PAGE
1-1	Fundamental-Mode Fields for Three Practical Dielectric Resonator Configurations	9
2-1	Dimensions and Coordinates for Rectangular and Cylindrical Resonators	10
2-2	Ratio of Characteristic Impedances Z_{0a}/Z_{0d} at Plane Boundary Between Dielectric and Air Media, $\epsilon_r = 100$	12
2-3	Cylindrical Dielectric Resonator Center-Frequency Data for Fundamental Mode - Comparison of First-Order Solution with Measured Points Given by H. M. Schlicke	13
2-4	Cylindrical Resonator Within Magnetic-Wall Waveguide Boundary	14
2-5	Calculated and Measured Resonant Frequency Versus D/L, TiO_2 Resonator	17
3-1	Experimental Setup for Dielectric Resonator as a Band-Rejection Filter Element in Waveguide. Detector Connection for Reflection-Coefficient Measurement is Shown. Alternate Connection for Insertion-Loss Measurement Indicated	20
3-2	Resonant Frequency Versus Position of Sample in Transverse Plane of Waveguide	22

LIST OF TABLES

TABLE	TITLE	PAGE
3-1	Samples of Polycrystalline TiO_2 Dielectric Material	19
3-2	Dielectric Resonator as Band-Rejection Filter Transmission and Reflection Measurements	21
3-3	Sample No. 4 Resonator as Band-Rejection Filter f_0 and Q vs. Position in Waveguide	23

SECTION I

PURPOSE

This program is intended to study the feasibility of high-dielectric-constant materials as resonators in microwave filters, and to obtain design information for such filters. Resonator materials shall be selected that have loss tangents capable of yielding unloaded Q values comparable to that of waveguide cavities. The materials shall have dielectric constants of at least 75 in order that substantial size reductions can be achieved compared to the dimensions of waveguide filters having the same electrical performance.

SECTION II

ABSTRACT

The objectives of this applied research program on microwave dielectric-resonator filters are discussed. The problems to be overcome before the advantages of these filters can be realized are explained. One important problem, the frequency sensitivity of high-dielectric-constant materials, falls outside the scope of this program. However, development of a suitable material having a dielectric constant of about 100 is considered feasible.

First- and second-order analyses of dielectric resonators are given for rectangular and cylindrical shapes. The first-order solution assumes the surface of the dielectric resonator to be an open-circuiting (or magnetic) wall, while the second-order solution assumes boundary conditions that are more complex, yet subject to simple computation. The superiority of the second-order solution is shown by comparison of theoretical and experimental resonant-frequency data. However, a frequency discrepancy of about 10 per cent indicates that either the second-order solution requires further improvement, or that the assumed dielectric-constant value is in error, or both.

Resonant frequency and unloaded Q measurements were made on six cylindrical samples having a wide range of diameter to length ratios. The experimental techniques are described. The unloaded Q of six TiO_2 samples was measured and found to be about 7000 at S-band. Since these samples were not of the highest purity, even higher Q 's should be possible. The effect of waveguide wall proximity was studied experimentally, and curves are given showing the effect of sample position in the waveguide on resonant frequency.

SECTION III
CONFERENCES

1. On 10 July 1963 a conference was held at the Signal Corps laboratory. Those attending were J. Agrios, E. A. Mariani, and J. Charleton of the Signal Corps, and S. B. Cohn of Rantec Corp. Objectives and plans for the program were discussed.
2. On October 7, E. A. Mariani of the Signal Corps and S. B. Cohn, C. W. Chandler, and K. C. Kelly of Rantec met at Rantec Corp. Results of the first quarter were reviewed, and future plans were discussed.

SECTION IV

FACTUAL DATA

1. Introduction

It has been known for many years that dielectric objects with free-space boundaries can resonate in various modes.^{1, 2, 3} If the dielectric constant of the object (dielectric resonator) is high, the electric and magnetic fields of a given resonant mode will be confined in and near the resonator, with the external fields attenuating to negligible values in a distance small compared to a free-space wavelength. Therefore, the radiation loss will be very small, and the unloaded Q , Q_u , of the resonance will be limited mainly by losses in the dielectric resonator. In materials of interest, the magnetic permeability is unity and magnetic losses are zero. Electric-field losses occur as a result of the finite loss tangent ($\tan \delta$) of the dielectric material. If all of the electric energy of the resonant mode is stored inside the dielectric resonator, and if no losses occur due to external fields, the unloaded Q will be given by $Q_u = 1/\tan \delta$. In the case of finite dielectric constant (ϵ_r), there will always be external loss due to radiation or dissipation in a surrounding metal shield. These losses will tend to reduce Q_u , while external electric stored energy will tend to increase Q_u . For ϵ_r of the order of 100 or higher, these effects will be small, and $Q_u \approx 1/\tan \delta$ appears to be a fair approximation. Typical $\tan \delta$ values for materials of interest range from about 0.0001 to 0.0003. Therefore Q_u values of about 3000 to 10,000 may be expected. These Q_u values are of the same order as those obtained with rectangular waveguide cavities.

The study program described in this First Quarterly Report has the objectives of exploring the feasibility of dielectric resonators in microwave filters and of obtaining the design data necessary for practical development of these filters. In order for dielectric resonators to be of value,

they must offer one or more advantages over conventional waveguide, coaxial, and strip-line resonators. Because the unloaded Q of dielectric resonators is approximately the same as that of waveguide cavity resonators, the selectivity and dissipation-loss characteristics obtainable in filters containing either kind of resonator will be approximately the same. Thus, the dielectric resonator filter must offer an advantage other than that of electrical performance in order to be justified. As the following discussion will show, a substantial size (and weight) advantage appears likely, and it is primarily on this basis that dielectric resonators are of interest.

For the fundamental-mode resonance, the dimensions of a dielectric resonator are on the order of one wavelength in the dielectric material. Since

$$\lambda_d = \frac{\lambda_a}{\sqrt{\epsilon_r}}$$

where λ_d is wavelength in the dielectric, λ_a is wavelength in air, and ϵ_r is relative dielectric constant, the resonator dimensions will be very small compared to λ_a if ϵ_r is large. For example, pure polycrystalline titanium dioxide (TiO_2) has a dielectric constant of about 100, so that $\lambda_d \approx 0.1\lambda_a$. Because the dimensions of an ordinary air-filled waveguide cavity are of the order of λ_a , it may be seen that a dielectric resonator can be much smaller than a waveguide cavity. It should be realized, however, that a dielectric resonator must have a metal enclosure around it to prevent radiation loss. The enclosure should be sufficiently larger than the dielectric resonator so that current induced on the metallic surface by the external field of the resonator will not seriously affect the unloaded Q of the resonator. Tentatively, it is believed that the enclosure's linear dimensions will have to be about twice those of the dielectric resonator. If that is the case, the reduction in size compared to ordinary waveguide cavities will be by approximately the factor $2/\sqrt{\epsilon_r}$. Thus, for TiO_2 , the linear dimensions of the dielectric resonator including its enclosure will

be about one-fifth that of a simple waveguide cavity. This is a very considerable size advantage.

It must not be ignored that the dimensions of a dielectric resonator may be as large or larger than those of a capacitively loaded waveguide cavity, a coaxial resonator, or a helical resonator. The Q_u of these resonators, however, would be lower in the microwave range. For example, at 10,000 Mc a TiO_2 resonator might typically be about 0.13 inch in diameter by 0.06 inch thick, and the enclosure approximating a cube 0.25 inch on each side. A strip-line or coaxial quarter-wave air-filled resonator occupying that volume would have a practical Q_u of about 1400. At 1000 Mc the dimensions would be about 2.5 x 2.5 x 2.5 inch and the Q_u of a strip-line or coaxial resonator about 4500. These Q_u values should be compared to 5000 to 10,000 for TiO_2 resonators of high purity. The advantage of the dielectric resonator is most striking at the higher microwave frequencies, and appears to be marginal near 1000 Mc. Below 500 Mc, capacitively loaded strip-line and coaxial resonators have the advantage.*

A disadvantage of dielectric resonators as compared to conventional resonators is variation of dielectric constant with temperature. For TiO_2 the relative change of dielectric constant is 800 ppm per $^{\circ}C$ (800 parts per million per degree Centigrade). Since resonant frequency is proportional to $1/\sqrt{\epsilon_r}$, the relative frequency change will be 400 ppm per $^{\circ}C$. Higher dielectric constant materials such as strontium titanate ($\epsilon_r \approx 230$) and barium titanate ($\epsilon_r > 1000$) have much greater temperature

*An even smaller resonator offering an unloaded Q in the thousands at frequencies above 2000 Mc is the single-crystal yttrium-iron-garnet (YIG) sphere. The individual resonators can be on the order of 0.050 inch in diameter. However, a magnetic field of extreme uniformity must be provided. The complete filter including its magnet is not likely to have a size and weight advantage. YIG-sphere filters have their particular advantage when electronic tunability is desired.

sensitivities. In contrast, a brass waveguide cavity has an expansion coefficient of 20 ppm per $^{\circ}\text{C}$, and invar, 1 ppm per $^{\circ}\text{C}$. Since resonant frequency is inversely proportional to linear dimensions, the frequency sensitivities have the same values. Thus the frequency sensitivities of brass and invar cavities are one-twentieth and one-four-hundredth the value for TiO_2 resonators, respectively.

As an example of temperature sensitivity, an X-band band-pass filter utilizing TiO_2 resonators would have a center-frequency shift of 4 Mc per $^{\circ}\text{C}$. For most applications this cannot be tolerated. Therefore, a materials study is required leading to a practical material having parameters on the order of $\epsilon_r = 100$, $\tan \delta = 0.0001$, and $\Delta\epsilon_r/\epsilon_r = 40(10)^{-6}$ per $^{\circ}\text{C}$, or better. A materials development program is not within the scope of the present program. However, before the results of this program can be applied to the design of filters for field applications, a material such as that specified above must be made available. Although a suitable material is not yet known to exist, its development, with an ϵ_r of about 100, is considered feasible by dielectric-material specialists of the Signal Corps laboratories. Successful development of a suitable material having ϵ_r substantially greater than 100 is not considered likely. For this reason, the present intention in this program is to concentrate experimental work on polycrystalline samples of TiO_2 , which are readily obtainable, and which have the desired values of ϵ_r and $\tan \delta$.

A basic understanding of dielectric resonators and a physical picture of their modal fields may be obtained in an approximate way by considering the dielectric resonator with an air boundary to be the dual of conventional metal-wall resonators. Since the metal walls of the latter act as short-circuiting boundaries, duality requires the dielectric resonator surfaces to act as open-circuiting boundaries. This will be true in a rough way if the dielectric constant is high, since in that case the characteristic impedance of the dielectric medium will be generally small compared to that of the air medium. The assumption is not perfect, as

it fails at certain angles of incidence of the wave impinging on the boundary, but it is sufficiently good for qualitative conclusions. An analysis of cylindrical resonators utilizing this assumption has been made by Schlicke². A more accurate "second-order" solution in which the external fields are taken approximately into account has been obtained by Okaya and Barash³. Their analysis was made for rectangular resonators, but may also be applied to cylindrical shapes, as shown in Section 2 of this report. Exact solutions are possible only for dielectric resonators with surfaces conforming to complete wave surfaces in three-dimensional coordinate systems yielding explicit wave functions. Thus, rigorous solutions for spherical, toroidal, and ellipsoidal resonators are feasible, while solutions for finite cylindrical and rectangular resonators are not. The first two cases were treated by Richtmeyer¹.

When two structures are duals, their E and H fields may be interchanged. Thus, the field configurations in the cases of fundamental modes in rectangular and cylindrical dielectric resonators are inferred from their metal-walled counterparts to be as shown in Figure 1-1. Note that the H-field of these modes traverses the inside of the resonators without changing sign or going to zero. In a metal-walled cavity, only the E-field can behave in this manner. Note further that there is an external H-field (and also an external E-field) appropriate to that of a magnetic dipole. As mentioned earlier, if ϵ_r is large this external field decays rapidly with distance from the resonator, and radiation loss is small.

The effect of anisotropy of the dielectric constant must also be considered. In most single crystals dielectric constant is a function of direction. As shown by Okaya and Barash³, the number of modes is doubled for anisotropic media such as single-crystal TiO_2 , as compared to isotropic media. In general, each mode of the isotropic medium is split into two different modes in single-crystal TiO_2 . If the physical axis is not properly aligned to the optical axis, the situation might be even worse. Thus, for filters it is highly desirable to use isotropic materials in order to minimize difficulties

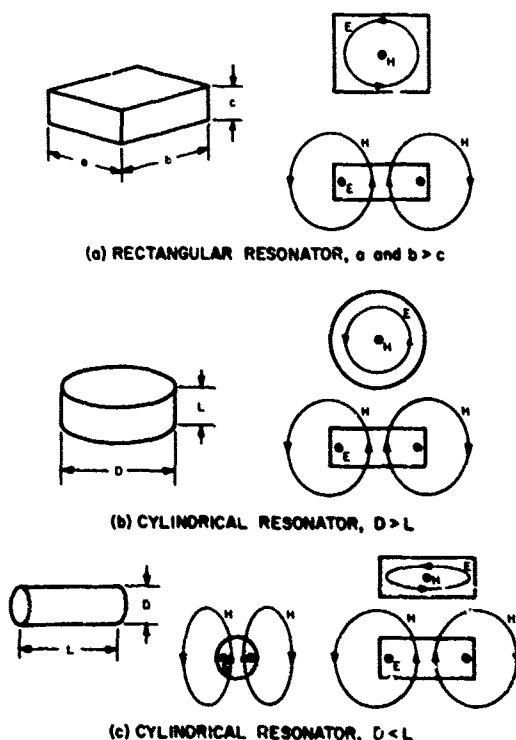


Figure 1-1. Fundamental-Mode Fields for Three Practical Dielectric Resonator Configurations

cover such topics as microwave measurements of ϵ_r , magnetic dipole moment of dielectric resonators, problems of coupling, tuning and shielding, design information for band-pass and band-rejection filters, and construction techniques.

2. First- and Second-Order Analysis of Dielectric Resonators

a. First-Order Solution

As a first-order approximation in computing the internal fields, the surface of a high-dielectric-constant resonator may be assumed

due to spurious responses. Other reasons for using isotropic polycrystalline materials are the difficulty involved in cutting the surfaces in accurate relationship to the optical axis, and the scarcity and expense of large single-crystal samples of high quality. Unless it should prove that polycrystalline materials are significantly lossier than single-crystal materials, the former will be used exclusively in this program.

In this First Quarterly Report, a general "second-order" solution applying to variously shaped resonators is derived. This is compared to experimental data obtained for cylindrical resonators. Preliminary Q_u data are also given. Future reports on this program will

to be an infinite-impedance boundary (or magnetic wall). Subject to this approximation, the fields in the resonator are exact duals of the fields in a metal-walled resonator of the same size and shape filled with a medium $\epsilon'_r = \mu_r = 1$ and $\mu'_r = \epsilon_r$. Thus, $E' = \eta H$ and $H' = -E/\eta$, where primed quantities apply to the metal-walled medium, unprimed quantities to the magnetic-walled dielectric resonator, and $\eta = \sqrt{\mu_0/\epsilon_0} = 377$ ohms. The resonant frequencies of the corresponding dual modes are equal. In designating the modes, TE_{lmn} and TM_{lmn} for the metal-walled resonator become TM_{lmn} and TE_{lmn} for the magnetic walled medium, where TE indicates that the electric field lies in planes transverse to the z-axis, and TM indicates the same for the magnetic field. Thus, for the rectangular magnetic-walled resonator in Figure 2-1(a), the fundamental (or lowest frequency) mode is the TE_{110} mode. For the cylindrical resonator in Figure 2-1(b), the fundamental mode is the TE_{010} mode when $L < D$, and the TM_{111} mode when $L > D$. The fields for these modes are sketched in Figure 1-1. Formulas for the resonant wavelengths of the metal-walled dual resonators may be found in numerous texts.

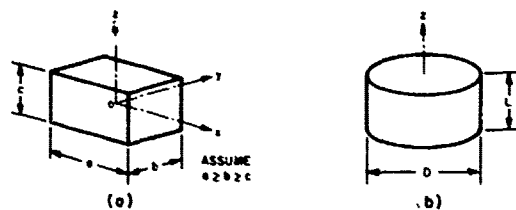


Figure 2-1. Dimensions and Coordinates for Rectangular and Cylindrical Resonators

b. Impedance Discontinuity on an Infinite Plane Boundary

Obviously, the accuracy of the first-order solution must be mediocre, since substantial field energy exists outside of the dielectric resonator. Thus, the surface must be a poor substitute for an open circuit. An analysis of the characteristic impedance ratio Z_{oa}/Z_{od} is of interest in this regard, (Z_{oa} and Z_{od} are characteristic impedances in the air and dielectric media evaluated for corresponding directions of uniform plane-wave

propagation designated by angles θ_d and θ_a measured from the normal to the surface). The characteristic impedances are defined in the usual way,⁴ being the ratio of the E and H components in planes parallel to the surface. The angles θ_d and θ_a are related as follows by Snell's law.

$$\sin \theta_a = \sqrt{\epsilon_r} \sin \theta_d \quad (2-1)$$

Note that $\theta_a = 90^\circ$ when $\theta_d = \sin^{-1}(1/\sqrt{\epsilon_r})$, and θ_a does not exist as a real angle for larger θ_d . The significance of this fact is that wave propagation in the air region is replaced by attenuation for $\theta_d \geq \sin^{-1}(1/\sqrt{\epsilon_r})$. The air-region attenuation constant in the direction of the normal is as follows:

$$\alpha_a = \frac{2\pi}{\lambda_a} \sqrt{\epsilon_r \sin^2 \theta_d - 1} \quad (2-2)$$

where the units of α_a are nepers per unit length, the length unit being that of λ_a , the wavelength in air.

In computing Z_{oa}/Z_{od} , there are two basic cases to consider; namely, E perpendicular to the plane of incidence (E_\perp) and E parallel to the plane of incidence (E_\parallel). The various formulas of interest for these two cases are as follows.⁴

E_\perp :

$$Z_{od} = \frac{\eta}{\sqrt{\epsilon_r}} \sec \theta_d \quad (2-3)$$

$$Z_{oa} = \eta / \sqrt{1 - \epsilon_r \sin^2 \theta_d} \quad (2-4)$$

$$\frac{Z_{oa}}{Z_{od}} = \frac{\sqrt{\epsilon_r} \cos \theta_d}{\sqrt{1 - \epsilon_r \sin^2 \theta_d}} \quad (2-5)$$

E_{\parallel} :

$$Z_{od} = \frac{\eta}{\sqrt{\epsilon_r}} \cos \theta_d \quad (2-6)$$

$$Z_{oa} = \eta \sqrt{1 - \epsilon_r \sin^2 \theta_d} \quad (2-7)$$

$$\frac{Z_{oa}}{Z_{od}} = \frac{\sqrt{\epsilon_r} \sqrt{1 - \epsilon_r \sin^2 \theta_d}}{\cos \theta_d} \quad (2-8)$$

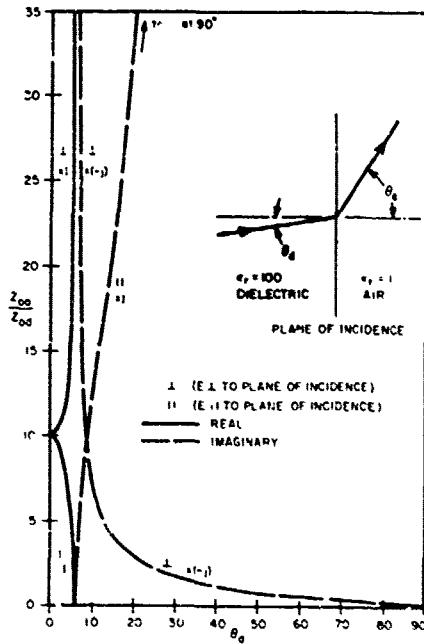


Figure 2-2. Ratio of Characteristic Impedances Z_{oa}/Z_{od} at Plane Boundary Between Dielectric and Air Media, $\epsilon_r = 100$

Equations 2-5 and 2-8 are plotted in Figure 2-2 for $\epsilon_r = 100$. The characteristic impedance Z_{oa} and the ratio Z_{oa}/Z_{od} are real for $\theta_d < 5.7^\circ$ and imaginary for $\theta_d > 5.7^\circ$. Thus propagation of energy through the boundary occurs below 5.7° while total reflection occurs above 5.7° . In the E_{\parallel} case, $|Z_{oa}/Z_{od}|$ is much larger than unity everywhere except very near $\theta_d = 5.7^\circ$. Thus, the E_{\parallel} case approximates an open-circuit boundary quite well. This is not true of the E_{\perp} case, however, since in most of the θ_d range $|Z_{oa}/Z_{od}|$ is quite small. The magnitude $|Z_{oa}/Z_{od}|$ is infinite at $\theta_d = 5.7^\circ$ and then drops monotonically to zero at $\theta_d = 90^\circ$. Above $\theta_d = 45^\circ$, $|Z_{oa}/Z_{od}|$ is less than one, and therefore the boundary approximates a short circuit rather than an open circuit. The reason for the poor accuracy of the first-order solution is now apparent. This is especially true in the case of the fundamental mode, since the first-order fields

of that mode can be represented by uniform plane waves propagating in various directions perpendicular to the z -axis. On the narrow walls parallel to the z -axis, the polarization of incidence is E_{\parallel} , so that the open-circuit approximation is quite good. However, on the broad walls perpendicular to the z -axis, the polarization of incidence is E_{\perp} with $\theta_d = 90^\circ$. Thus, $|Z_{oa}/Z_{od}| = 0$, and the first-order approximation breaks down completely.

The behavior of the experimental data in Figure 2-3 should now be clear. When D/L approaches zero, the area of the surfaces normal to the z -axis becomes negligible compared to the area of the other surfaces. Thus, the open-circuit approximation holds quite well over most of the total surface, with the result that the first-order solution has good accuracy. For D/L large, the opposite prevails, and the accuracy is very poor. Even for $D/L = 1$, the error is too great for the first-order solution to be useful.

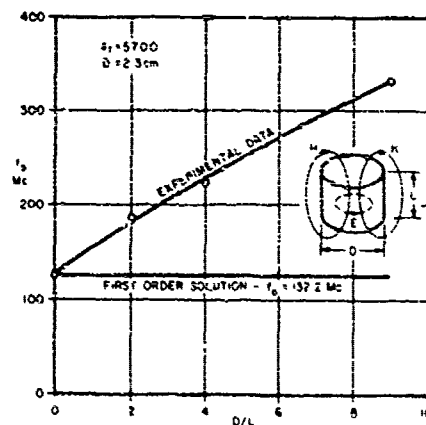


Figure 2-3. Cylindrical Dielectric Resonator Center-Frequency Data for Fundamental Mode - Comparison of First-Order Solution with Measured Points Given by H. M. Schlicke

c. Second-Order Solution

A more complex boundary-impedance assumption has been used by Okaya and Barash³ that yields greatly improved accuracy. With reference to Figure 2-1, they assume magnetic walls on the surfaces parallel to the z -axis, while on the surfaces perpendicular to the z -axis, they assume reactive terminations appropriate to the field distribution on these surfaces. More specifically, the Okaya and Barash boundary conditions are represented exactly by Figure 2-4, where the dielectric resonator is contained in a magnetic-wall waveguide. Thus, the dielectric-resonator problem is reduced

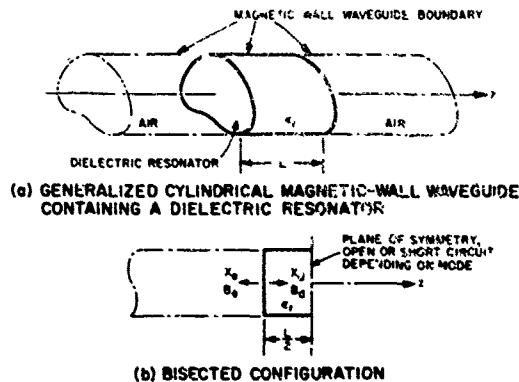


Figure 2-4. Cylindrical Resonator within Magnetic-Wall Waveguide Boundary

to a straightforward waveguide problem. Okaya and Barash confined their attention to rectangular resonators and did not utilize the waveguide model. The analysis given below in terms of a waveguide model should be more easily comprehended by microwave engineers and at the same time will yield a useful physical understanding of the problem.

The waveguide cross-section shape in Figure 2-4(a) is arbitrary.

In order to compute the resonant frequency of the resonator, it is merely necessary to know the cutoff wavelength of the waveguide cross-section. When the field functions of the resonant mode are desired, the waveguide-mode fields must be known in addition to the cutoff wavelength. By duality considerations, the cutoff wavelength and field functions are immediately known for the magnetic-walled waveguide if these quantities are known for a metal-walled waveguide having the same cross-section.

The resonant-mode solution is most easily obtained by applying the resonance condition

$$B_a + B_d = 0 \quad (2-9)$$

at the air-dielectric boundary of the bisected configuration in Figure 2-4(b). The plane of symmetry should be replaced by either a short-circuiting or open-circuiting terminating wall depending on the particular mode of resonance. For the fundamental TE mode, E_t (E transverse to z) is maximum at the plane of symmetry while H_t is zero. Therefore, an open-circuiting, or magnetic, wall is required in the plane of symmetry. The resonant

frequency occurs such that the dielectric-filled waveguide cross section is above cutoff. The propagation constant in the dielectric is equal to $j\beta_d = j2\pi/\lambda_{gd}$, where β_d is the wave constant. In the air-filled region, the cross section is below cutoff, and the propagation constant is equal to the attenuation constant, α_a . Here, and in the following analysis, subscript d denotes the dielectric-filled waveguide and subscript a the air-filled waveguide. The cutoff wavelengths are λ_{cd} and λ_{ca} in the two regions. Because λ_{cd} is a function only of the dimensions of the cross-section boundary and is independent of ϵ_r , one can write

$$\lambda_{cd} = \lambda_{ca} = \lambda_c. \quad (2-10)$$

Carrying through the waveguide analysis of Figure 2-4(b) for the TE mode one obtains*

$$B_a = Y_{oa}/j = \frac{1}{\eta} \frac{\lambda_{ga}}{\lambda_a} = -\frac{1}{\eta} \sqrt{\left(\frac{\lambda_a}{\lambda_c}\right)^2 - 1} \quad (2-11)$$

$$B_d = Y_{od} \tan \frac{\beta_d L}{2} \quad (2-12)$$

$$Y_{od} = \frac{\sqrt{\epsilon_r}}{\eta} \frac{\lambda_{gd}}{\lambda_d} = \frac{1}{\eta} \sqrt{\epsilon_r - \left(\frac{\lambda_a}{\lambda_c}\right)^2} \quad (2-13)$$

$$\beta_d = \frac{2\pi}{\lambda_{gd}} = \frac{2\pi}{\lambda_a} \sqrt{\epsilon_r - \left(\frac{\lambda_a}{\lambda_c}\right)^2} = \frac{2\pi\eta}{\lambda_a} Y_{od} \quad (2-14)$$

$$\alpha_a = \frac{2\pi}{\lambda_c} \sqrt{1 - \left(\frac{\lambda_c}{\lambda_a}\right)^2} = -\frac{2\pi\eta}{\lambda_a} B_a \quad (2-15)$$

*The analysis utilizes well-known waveguide relationships and definitions. A book such as Reference 4 may be used as background.

Now apply the resonance condition $B_a + B_d = 0$, and let λ_a equal λ_o , the resonant wavelength in air. The above equations yield

$$\tan \left(\frac{\beta_d L}{2} \right) = \frac{\alpha_a}{\beta_d} \quad (2-16)$$

$$\alpha_a = 2\pi \sqrt{\frac{1}{\lambda_c^2} - \frac{1}{\lambda_o^2}} \quad (2-17)$$

$$\beta_d = 2\pi \sqrt{\frac{\epsilon_r}{\lambda_o^2} - \frac{1}{\lambda_c^2}} \quad (2-18)$$

Before solving Equations 2-16 through 2-18 for λ_o , it is necessary to know λ_c for the cross section perpendicular to the z-axis. Utilizing waveguide theory and duality, one obtains the following relations for the TE modes of interest in magnetic walled waveguides.

$$\frac{1}{\lambda_c^2} = \frac{1}{4} \left(\frac{1}{a^2} + \frac{1}{b^2} \right) \quad (\text{TE}_{11} \text{ mode, rectangular cross-section}) \quad (2-19)$$

$$\frac{1}{\lambda_c^2} = \frac{0.585}{D^2} \quad (\text{TE}_{01} \text{ mode, circular cross-section}) \quad (2-20)$$

In using the second-order resonant-frequency equations when ϵ_r and the cross-section dimensions are given, it is convenient to assume a value of λ_o and then calculate the resonator length, L . Thus, $1/\lambda_c^2$ should be computed from Equation 2-19 or 2-20. Then α_a and β_d should be computed from Equations 2-17 and 2-18. Finally, Equation 2-16 may be solved explicitly for L .

d. Comparison of First- and Second-Order Solutions with Measured Data.

Figure 2-5 shows a comparison of computed resonant frequency curves and data taken on a series of TiO_2 cylindrical dielectric resonators of constant diameter $D = 0.400$ inch and varying L . The measurement technique is described in Section 3 of this report. Computed curves are shown for the first-order TE_{010} and TE_{011} modes, and the second-order TE_{016} mode. These modal designations are identical except for the third subscript in each case. By convention this subscript indicates the number of half-guide-wave-

length variations of field occurring in the z -direction within the resonator. For first-order modes, this subscript is an integer ≥ 0 . However, in the case of the second-order solution, this subscript is a non-integer given by

$$\delta = \frac{2L}{\lambda_g d} + \frac{3dL}{\lambda_g^2} \quad (2-19)$$

For the fundamental mode, δ falls between 0 and 1. (The value $\delta = 0$ implies open-circuit boundaries of the transverse resonator faces, while $\delta = 1$ implies short circuits at these faces.) This explains the computed curves in Figure 2-5, where the second-order TE_{016} curve lies between the first order TE_{010} and TE_{011} curves. The three curves have the same value at $L = \infty$ ($D/L = 0$), since $\lambda_g = \infty$ and the resonant frequency is simply the cut-off frequency of the dielectric-filled waveguide.

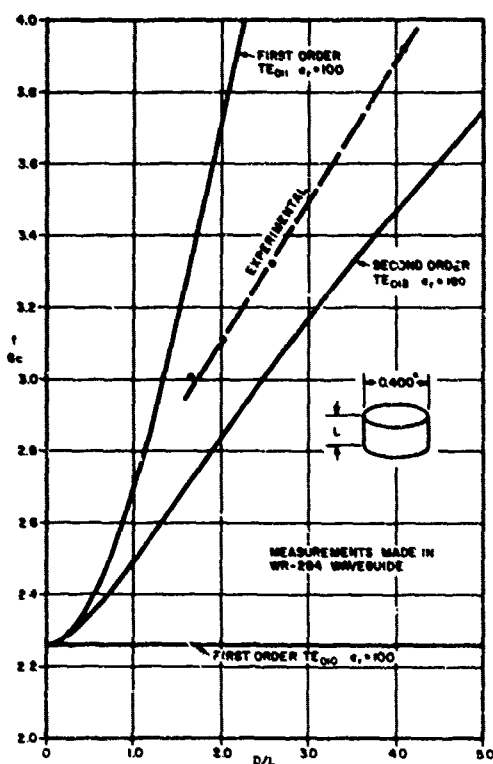


Figure 2-5. Calculated and Measured Resonant Frequency Versus D/L , TiO_2 Resonator

The experimental points in Figure 2-5 lie on a curve about 10 per cent in frequency above the TE_{010} curve, in the direction of the TE_{011} curve. There are two possible explanations for the disagreement between measured and calculated points. First, the true dielectric constant may differ from the assumed value of $\epsilon_r = 100$. A calculation has shown that a value $\epsilon_r = 83.8$ gives perfect agreement at 3.0 Gc, and a 2.5 per cent discrepancy at 3.8 Gc. A second explanation might be the effect of the difference between the true boundary conditions and the assumed boundary conditions of the second-order analysis.

As a further test of the second-order formulas, a TE_{010} point was computed for the graph in Figure 2-3. At $f_0 = 200$ Mc, the value $D/L = 6.80$ was found. This lies between the data and the first order TE_{010} curve, a situation opposite to that of Figure 2-5. The large discrepancy in this case is not understood; however, the extremely high $\epsilon_r = 5700$ value places this case far beyond the range of interest of this program.

The second-order solution is a definite improvement over either the first-order TE_{010} or TE_{011} solution. Its accuracy of about 10 per cent is adequate for preliminary design purposes.* As an aid in evaluating the causes of error, precise microwave measurements of ϵ_r will be made during the second quarter of this program. After the ϵ_r data are available, further study may reveal how the accuracy of the second-order solution may be improved.

*Figure 6 of Okaya and Barash indicates almost perfect agreement of the second-order solution with fundamental-mode frequencies measured on rectangular dielectric resonators. Although anisotropic single-crystal specimens were used, the orientation of the E field was such that an isotropic dielectric constant, $\epsilon_r = 78.3$, could be assumed in the case of the fundamental TE_{110} mode. However, our own calculations for this case disagree with those of Okaya and Barash, and indicate that the experimental points lie about six per cent in frequency above the theoretical curve. The discrepancy is thus similar to that in Figure 2-5. Again, either the assumed ϵ_r value or the boundary conditions, or possibly both, may be at fault.

3. Measurements on Cylindrical Dielectric Resonators

At the start of the program, six samples of polycrystalline TiO_2 dielectric material were available, as listed in Table 3-1.

TABLE 3-1
SAMPLES OF POLYCRYSTALLINE TiO_2
DIELECTRIC MATERIAL

Sample No.	Diameter	Length
1	0.400 in.	0.255 in.
2	0.400	0.255
3	0.400	0.241
4	0.400	0.198
5	0.400	0.155
6	0.400	0.090

These initial samples were supplied by the Signal Corps, and were not claimed to be of particularly good quality. The samples were employed in some experiments of a preliminary nature as described below.

An experimental setup for testing samples as band-rejection elements is shown in Figure 3-1. At resonance nearly all the incident energy is reflected and the transmitted energy exhibits a deep null. The sample is supported on polyfoam in WR-284 waveguide, with the axis of the sample parallel to the transverse magnetic field of the TE_{10} mode in the waveguide. The setup as shown permits measurement of reflection and transmission coefficients vs. frequency. Automatic sweep and oscilloscope display were used to locate resonances and observe general characteristics. The rejection resonances were then investigated in detail to determine resonant frequency, bandwidth, and insertion loss. The loaded Q , Q_L , can be determined from the resonant frequency and bandwidth data. Then the unloaded Q , Q_u , can be determined from Q_L and the peak insertion-loss value at resonance, L_p .

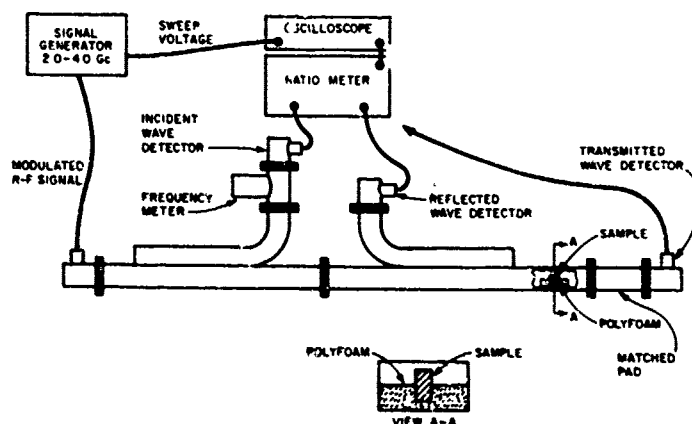


Figure 3-1. Experimental Setup for Dielectric Resonator as a Band-Rejection Filter Element in Waveguide. Detector Connection for Reflection-Coefficient Measurement is Shown. Alternate Connection for Insertion-Loss Measurement is Indicated.

Since this data can be computed from either the transmission or reflection coefficient response, measurements were made on both. The data obtained from the above experiments are shown in Tables 3-2 and 3-3, and in Figure 2-5. Reflection and transmission bandwidths were measured at the 3-, 6-, and 10-db points. The Q_L values are calculated by dividing the resonant frequency by the bandwidth times an appropriate factor based on a simple resonant-circuit response. This factor is unity for a 3-db bandwidth. The factors are tabulated below for both transmission and reflection.

	Bandwidth Factor		
	3 db	6 db	10 db
Transmission	1.0	0.577	0.333
Reflection	1.0	1.732	3.000

The Q_u value is calculated from Q_L and L_p . In principle, Q_u can also be determined from the reflection coefficient at resonance rather than from L_p , but the former is too close to unity to be measured accurately. For transmission through a band-rejection resonator at resonance, the insertion loss L_p is

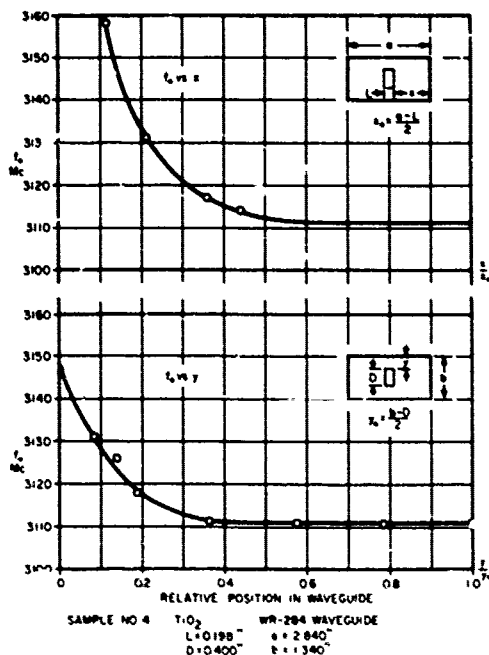
$$L_p = 20 \log_{10} \left(\frac{Q_u}{Q_L} \right) \text{ db.} \quad (3-1)$$

From the tabulated data in Table 3-2 one can see that the Q_L values determined from transmission data are lower and less consistent than those

TABLE 3-2
DIELECTRIC RESONATOR AS BAND-REJECTION FILTER
TRANSMISSION AND REFLECTION MEASUREMENTS

Sample	f_o Mc	3db BW Mc	Q_L	6db BW Mc	Q_L	10db BW Mc	Q_L	Avg Q_L	L_o db	Q_u
TRANSMISSION MEASUREMENTS										
1	2937	30	98	18	94	11	89	94	35.0	6426
2	2925	28	102	17	99	10	97	100	35.5	6923
3	3005	30	100	18	96	10	100	99	35.5	7001
4	3111	31	100	18	100	11	94	98	36.0	7458
5	3320	34	98	20	96	11	101	98	36.5	7778
6	3918	37	106	24	94	13	100	100	36.5	6693
REFLECTION MEASUREMENTS										
1	2936	26	113	44	116	77	114	114		
2	2924	25	117	43	118	77	114	116		
3	3005	25	120	44	118	79	114	118		
4	3111	26	120	45	120	81	115	118		
5	3320	28	119	49	117	88	113	116		
6	3918	35	112	61	111	108	109	111		

from reflection data. This is believed to be the result of the bandwidth being measured at points 3-, 6-, and 10-db down from the available generator power that is, measured with respect to zero insertion loss. The configuration was not matched off resonance in this experiment, and the entire insertion-loss response curve was raised above 0 db. Therefore, the measured bandwidths are broader than the true 3-, 6-, and 10-db bandwidths. The reflection bandwidths are considered more accurate, and the resulting Q_L 's are used in the computation of Q_u . It can also be seen from the data that the value of Q_u is quite sensitive to error in insertion-loss measurement. This measurement is difficult to make accurately due to the large value of insertion loss and the sharpness of the resonant rejection peak. The latter requires a signal source with good frequency stability and no frequency modulation.



A second experiment consisted of determining the effect of moving a sample toward the broad and narrow walls of the waveguide. Sample No. 4 was used in this test. The data are shown in Figure 3-2 and Table 3-3. Transmission data only was taken in this experiment, so that the Q_L values are probably lower than actual for the reasons previously described. This in turn lowers the calculated Q_u values.

Figure 3-2. Resonant Frequency Versus Position of Sample in Transverse Plane of Waveguide

TABLE 3-3

SAMPLE NO. 4 RESONATOR AS BAND-REJECTION FILTER
 f_o AND Q VS. POSITION IN WAVEGUIDE

x/x_o	f_o , Mc	3db BW Mc	Q_L	6db BW Mc	Q_L	10db BW Mc	Q_L	Avg Q_L	L_o , db	Q_u
0.114	3158	4	790						15.5	4700
0.212	3131	5	616						20.2	6300
0.360	3117	10	318						26.5	6740
0.436	3114	15	208						28.5	5540
1.00	3111	31	100						36.0	6320
y/y_o										
0	3147	35	89.0	20	89.9	11	94.3	91	36.0	5745
0.085	3131	32	97.2	18	99.8	11	94.3	97	36.5	6480
0.138	3126	29	107.2	18	99.6	10	104.7	104	36.5	6950
0.191	3118	31	100.6	18	100	11	94.4	98		
0.352	3111									
0.574	3110									
0.786	3110									
1.00	3110	32	97.2	19	94.5	11	94.3	95	36.0	6000

SECTION V

CONCLUSIONS

Dielectric resonators in microwave filters are capable of unloaded Q's comparable to those of conventional waveguide cavities. A substantial size reduction is possible compared to waveguide filters yielding the same electrical performance. The higher the dielectric constant, the smaller will be the filter; however, dielectric constants higher than 100 are not likely to be practical because of excessive temperature sensitivity. Even materials of $\epsilon_r \approx 100$ are not yet suitable from this standpoint, but it is believed that such a material can be developed to have a resonant frequency vs. temperature stability comparable to ordinary waveguide cavities. Work on this program will concentrate on readily available TiO_2 samples, since these have the desired dielectric constant and low losses. Isotropic, polycrystalline specimens will be used in order to avoid the resonant-frequency splitting of anisotropic single crystals.

The study of the first- and second-order solutions show the latter to be much superior to the former. Experimental data indicate that further analytical improvement may be needed.

Experimental techniques of measurement utilizing the dielectric samples as band-rejection elements were found satisfactory. The Q_u of a series of TiO_2 samples was on the order of 7000 at S-band. Considering that the samples were not of high purity, this value of Q is very good. Metal-wall proximity experiments confirmed expectations that the external fields attenuate rapidly, and that the metal shield around a resonator or group of resonators need not be very large.

SECTION VI
PROGRAM FOR NEXT INTERVAL

Techniques of measuring ϵ_r of cylindrical samples will be developed and used to obtain accurate data. This will make possible a more precise evaluation of the second-order solution.

An analysis will be made of the equivalent magnetic dipole moment of a resonator. Coupling formulas will be developed that utilize the magnetic dipole moment.

Experimental studies will be made of coupling between resonators in a metal waveguide below cutoff. Coupling to terminating waveguide and coaxial lines will be investigated.

SECTION VII

LIST OF REFERENCES

1. R. D. Richtmeyer, Journ. of Appl. Phys., Vol. 10, p. 391; 1939.
2. H. M. Schlicke, "Quasi-Degenerated Modes in High- ϵ Dielectric Cavities," Journ. of Appl. Phys., Vol. 24, pp. 187-191; Feb., 1953.
3. A. Okaya and L. F. Barash, "The Dielectric Microwave Resonator," Columbia Radiation Laboratory Report, Columbia University, New York, N. Y. Also, Proc. IRE, Vol. 50, pp. 2081-2092; Oct. 1962.
4. S. Ramo and J. R. Whinnery, "Fields and Waves in Modern Radio," 2nd Ed., pp. 296-301; John Wiley and Sons, Inc., New York, 1953.

SECTION VIII
IDENTIFICATION OF KEY TECHNICAL PERSONNEL

	Hours
Dr. Seymour B. Cohn Specialist	40
Mr. Charles W. Chandler Senior Engineer	220
Mr. Kenneth C. Kelly Senior Engineer	16
Mr. Richard V. Reed Engineer	12

AD	DIV	UNCLASSIFIED	AD	DIV	UNCLASSIFIED
Rantec Corporation, Calabasas, California	MICROWAVE DIELECTRIC-RESONATOR FILTERS, by S. B. Cohn and C. W. Chandler, an investigation. First Quarterly Report, 1 July to 30 September 1963, 28p. incl. illus., tables, 4 refs. (Rept. no. 1, proj. 31625) (Contract DA 36-039-AMC-02267(E)) uncl.	<p>I. Dielectric-Resonator Filters -- Analyses</p> <p>I. Title: Microwave Dielectric-Resonator Filters</p> <p>II. Cohn, S. B. and Chandler, C. W.</p> <p>III. Rantec Corp., Calabasas, Calif.</p> <p>IV. Contract DA 36-039-AMC-02267(E)</p>	Rantec Corporation, Calabasas, California	MICROWAVE DIELECTRIC-RESONATOR FILTERS, by S. B. Cohn and C. W. Chandler, an investigation. First Quarterly Report, 1 July to 30 September 1963, 28p. incl. illus., tables, 4 refs. (Rept. no. 1, proj. 31625) (Contract DA 36-039-AMC-02267(E)) uncl.	<p>I. Dielectric-Resonator Filters -- Analyses</p> <p>I. Title: Microwave Dielectric-Resonator Filters</p> <p>II. Cohn, S. B. and Chandler, C. W.</p> <p>III. Rantec Corp., Calabasas, Calif.</p> <p>IV. Contract DA 36-039-AMC-02267(E)</p>
	The objectives of this applied research program are discussed. One important problem, the frequency sensitivity of high-dielectric-constant materials, falls outside the scope of this program. However, a suitable material having a dielectric constant of about 100 is considered feasible. First- and second-order analyses are given for rectangular and cylindrical.	ASTIA		The objectives of this applied research program are discussed. One important problem, the frequency sensitivity of high-dielectric-constant materials, falls outside the scope of this program. However, a suitable material having a dielectric constant of about 100 is considered feasible. First- and second-order analyses are given for rectangular and cylindrical.	ASTIA
AD	DIV	UNCLASSIFIED	AD	DIV	UNCLASSIFIED
Rantec Corporation, Calabasas, California	MICROWAVE DIELECTRIC-RESONATOR FILTERS, by S. B. Cohn and C. W. Chandler, an investigation. First Quarterly Report, 1 July to 30 September 1963, 28p. incl. illus., tables, 4 refs. (Rept. no. 1, proj. 31625) (Contract DA 36-039-AMC-02267(E)) uncl.	<p>I. Dielectric-Resonator Filters -- Analyses</p> <p>I. Title: Microwave Dielectric-Resonator Filters</p> <p>II. Cohn, S. B. and Chandler, C. W.</p> <p>III. Rantec Corp., Calabasas, Calif.</p> <p>IV. Contract DA 36-039-AMC-02267(E)</p>	Rantec Corporation, Calabasas, California	MICROWAVE DIELECTRIC-RESONATOR FILTERS, by S. B. Cohn and C. W. Chandler, an investigation. First Quarterly Report, 1 July to 30 September 1963, 28p. incl. illus., tables, 4 refs. (Rept. no. 1, proj. 31625) (Contract DA 36-039-AMC-02267(E)) uncl.	<p>I. Dielectric-Resonator Filters -- Analyses</p> <p>I. Title: Microwave Dielectric-Resonator Filters</p> <p>II. Cohn, S. B. and Chandler, C. W.</p> <p>III. Rantec Corp., Calabasas, Calif.</p> <p>IV. Contract DA 36-039-AMC-02267(E)</p>
	The objectives of this applied research program are discussed. One important problem, the frequency sensitivity of high-dielectric-constant materials, falls outside the scope of this program. However, a suitable material having a dielectric constant of about 100 is considered feasible. First- and second-order analyses are given for rectangular and cylindrical.	ASTIA		The objectives of this applied research program are discussed. One important problem, the frequency sensitivity of high-dielectric-constant materials, falls outside the scope of this program. However, a suitable material having a dielectric constant of about 100 is considered feasible. First- and second-order analyses are given for rectangular and cylindrical.	ASTIA

AD	DIV	UNCLASSIFIED	AD	DIV	UNCLASSIFIED
drical shapes. The first-order solution assumes the surface of the dielectric resonator to be an open-circuiting (or magnetic) wall, while the second-order solution assumes boundary conditions that are more complex. The superiority of the second-order solution is shown by comparison of theoretical and experimental resonant-frequency data. However, a frequency discrepancy of about 10 per cent remains to be explained. The unloaded Q of six TiO ₂ samples was measured and found to be about 7000 at S-band. Since these samples were not of the highest purity, even higher Q's should be possible. The effect of waveguide wall proximity on resonant frequency was studied experimentally.	UNTERMS Filters Dielectric-Constant Resonator Cylindrical Rectangular Isotropic Magnetic-Dipole Magnetic-Wall Microwave Mode Q TiO ₂	drical shapes. The first-order solution assumes the surface of the dielectric resonator to be an open-circuiting (or magnetic) wall, while the second-order solution assumes boundary conditions that are more complex. The superiority of the second-order solution is shown by comparison of theoretical and experimental resonant-frequency data. However, a frequency discrepancy of about 10 per cent remains to be explained. The unloaded Q of six TiO ₂ samples was measured and found to be about 7000 at S-band. Since these samples were not of the highest purity, even higher Q's should be possible. The effect of waveguide wall proximity on resonant frequency was studied experimentally.	UNTERMS Filters Dielectric-Constant Resonator Cylindrical Rectangular Isotropic Magnetic-Dipole Magnetic-Wall Microwave Mode Q TiO ₂	UNCLASSIFIED	
AD	DIV	UNCLASSIFIED	AD	DIV	UNCLASSIFIED
drical shapes. The first-order solution assumes the surface of the dielectric resonator to be an open-circuiting (or magnetic) wall, while the second-order solution assumes boundary conditions that are more complex. The superiority of the second-order solution is shown by comparison of theoretical and experimental resonant-frequency data. However, a frequency discrepancy of about 10 per cent remains to be explained. The unloaded Q of six TiO ₂ samples was measured and found to be about 7000 at S-band. Since these samples were not of the highest purity, even higher Q's should be possible. The effect of waveguide wall proximity on resonant frequency was studied experimentally.	UNTERMS Filters Dielectric-Constant Resonator Cylindrical Rectangular Isotropic Magnetic-Dipole Magnetic-Wall Microwave Mode Q TiO ₂	drical shapes. The first-order solution assumes the surface of the dielectric resonator to be an open-circuiting (or magnetic) wall, while the second-order solution assumes boundary conditions that are more complex. The superiority of the second-order solution is shown by comparison of theoretical and experimental resonant-frequency data. However, a frequency discrepancy of about 10 per cent remains to be explained. The unloaded Q of six TiO ₂ samples was measured and found to be about 7000 at S-band. Since these samples were not of the highest purity, even higher Q's should be possible. The effect of waveguide wall proximity on resonant frequency was studied experimentally.	UNTERMS Filters Dielectric-Constant Resonator Cylindrical Rectangular Isotropic Magnetic-Dipole Magnetic-Wall Microwave Mode Q TiO ₂	UNCLASSIFIED	

UNITED STATES ARMY ELECTRONICS RESEARCH & DEVELOPMENT AGENCY
STANDARD DISTRIBUTION LIST
RESEARCH AND DEVELOPMENT CONTRACT REPORTS

	<u>Copies</u>
OASD (R & E), ATTN: Technical Library, Room 3E1065 The Pentagon, Washington 25, D.C.	1
Chief of Research and Development, OCS, Department of the Army, Washington, D.C. 20315	1
Commanding General, U. S. Army Materiel Command ATTN: R & D Directorate, Washington 25, D.C.	1
Commanding General, U. S. Army Electronics Command ATTN: AMSEL-AD, Fort Monmouth, New Jersey 07703	1
Director, U. S. Naval Research Laboratory ATTN: Code 2027, Washington, D.C. 20390	1
Commander, Aeronautical Systems Division, ATTN: ASNXRR Wright-Patterson Air Force Base, Ohio	1
Hq, Electronic Systems Division, ATTN: ESAL L. G. Hanscom Field, Bedford, Massachusetts	1
Commander, Air Force Cambridge Research Laboratories ATTN: CRO, L. G. Hanscom Field, Bedford, Massachusetts	1
Commander, Air Force Command & Control Development Division ATTN: CRZC, L. G. Hanscom Field, Bedford, Massachusetts	1
Commander, Rome Air Development Center, ATTN: RAALD Griffiss Air Force Base, New York	1
Commander, Defense Documentation Center, ATTN: TISIA Cameron Station, Building 5, Alexandria, Virginia 22314	10
Chief, U. S. Army Security Agency, Arlington Hall Station Arlington 12, Virginia	2
Deputy President, U. S. Army Security Agency Board Arlington Hall Station, Arlington 12, Virginia	1
Commanding Officer, Harry Diamond Laboratories ATTN: Library, Room 211, Building 92 Washington 25, D.C.	1
Director, USAEGIMRADA, ATTN: ENGGM-SS Fort Belvoir, Virginia 22060	1
AFSC Scientific/Technical Liaison Office, U. S. Naval Air Development Center, Johnsville, Pennsylvania	1
USAEIRD. Liaison Office, Rome Air Development Center ATTN: RAOL, Griffiss Air Force Base, New York 13442	1
Commanding Officer, U. S. Army Electronics Materiel Support Agency, ATTN: SELMS-ADJ, Fort Monmouth, New Jersey 07703	1

	<u>Copies</u>
Marine Corps Liaison Office, U. S. Army Electronics Research and Development Laboratory, ATTN: SELRA/LNR Fort Monmouth, New Jersey 07703	1
Commanding Officer, U. S. Army Electronics Research and Development Laboratory, ATTN: Director of Research or Engineering, Fort Monmouth, New Jersey 07703	1
Commanding Officer, U. S. Army Electronics Research and Development Laboratory, ATTN: Technical Documents Center, Fort Monmouth, New Jersey 07703	1
Advisory Group on Electron Devices, 346 Broadway New York, New York 10013	2
Commanding Officer, U. S. Army Electronics Research and Development Laboratory, ATTN: SELRA/TNR Fort Monmouth, New Jersey 07703	3

FOR RETRANSMITTAL TO ACCREDITED BRITISH AND CANADIAN
GOVERNMENT REPRESENTATIVES

Commanding General, U. S. Army Combat Developments Command ATTN: CDCMR-E, Fort Belvoir, Virginia 22060	1
Commanding Officer, U. S. Army Combat Developments Command Communications-Electronics Agency Fort Huachuca, Arizona 85613	1
Director, Fort Monmouth Office, U. S. Army Combat Developments Command, Communications-Electronics Agency, Building 410 Fort Monmouth, New Jersey 07703	1
AFSC Scientific/Technical Liaison Office, U. S. Army Electronics Research and Development Laboratory Fort Monmouth, New Jersey 07703	1
Commanding Officer and Director, U. S. Navy Electronics Laboratory, San Diego 52, California	1
	<u>41</u>

SUPPLEMENTAL DISTRIBUTION

Stanford Research Institute, ATTN: Dr. Matthaei Menlo Park, California	1
National Bureau of Standards, Engineering Electronics Section ATTN: Mr. Gustave Shapiro, Chief, Washington 25, D. C.	1
Chief, Bureau of Ships, Department of the Navy ATTN: Mr. Gumina, Code 68182, Washington 25, D. C.	1
Commander, Rome Air Development Center, ATTN: Mr. P. Romanelli RCLRA-2, Griffiss Air Force Base, New York	1
Commanding Officer, U. S. A. Electronics Research & Development Laboratory, Fort Monmouth, New Jersey	
ATTN: SELRA/PE (Division Director)	1
ATTN: SELRA/PE (Dr. E. Both)	1
ATTN: SELRA/PEM (Mr. N. Lipetz)	1
ATTN: SELRA/PEM (Mr. J. Charlton)	1
ATTN: SELRA/PEM (Mr. E. Mariani)	7